agronomy

MDPI

Article

Understanding the Effect of Seasonal Climate Variability on the Salinity in Unsaturated Agricultural Soil

Hongde Wang [1,2], Dongli She [2,3,*] and Rafaela Cardoso [4]

[1] School of Earth Sciences and Engineering, Hohai University, Nanjing 211100, China; whd1993@hhu.edu.cn
[2] Jiangsu Province Engineering Research Center for Agricultural Soil-Water Efficient Utilization, Carbon Sequestration and Emission Reduction, Nanjing 211100, China
[3] College of Agricultural Science and Engineering, Hohai University, Nanjing 210098, China
[4] CERIS/Instituto Superior Técnico, University of Lisbon, 1049-001 Lisbon, Portugal; rafaela.cardoso@tecnico.ulisboa.pt
* Correspondence: shedongli@hhu.edu.cn

Abstract: Salinization/desalinization processes in the soil vadose zone are important to define agricultural irrigation and drainage schedules, especially in reclaimed crop areas. Numerical modeling of soil–climate interaction is a very helpful tool to understand soil salinity distribution and solute transport and therefore define efficient desalination solutions. A finite element analysis program Code_Bright was used to perform a coupled thermo-chemo-hydraulic analysis aiming at investigating the effect of climate actions on the distribution of soil salinity in depth, by modeling solute transport in the vadose zone under fresh/saline groundwater supply. The analysis separated first the effect of rain infiltration and evaporation, and then a real climate was considered as the boundary condition. A downward flow pattern induced by rainfall in the unsaturated zone resulted in a nonlinear salt leaching process. Significant differences in salt concentration between the surface and lower layer caused by rainfall resulted in a decrement in the leaching efficiency. Evaporation causes water to move upward and salt transport to the surface, thus enhancing the soil salinity above the evaporation front. The salinity above the groundwater table and below the evaporation front were less affected regardless of the salinity of the supplied groundwater. The model simulated the salt leaching process during the wet seasons and salt accumulation processes during the dry ones. The soil salinity and saturation at the soil surface have significantly responded to seasonal climate variability. A typical seasonal climate variability would result in a low salt leaching efficiency through years in the coastal reclamation area. These results would be helpful for the design of soil salinization management strategies, such as reducing salt accumulation by reducing evaporation or leaching the surface salt in the dry season, and increasing the drainage to promote leaching in the wet season.

Keywords: soil salinization; climate actions; finite element analysis; coastal reclamation; vadose zone; soil–atmosphere interface

check for updates

Citation: Wang, H.; She, D.; Cardoso, R. Understanding the Effect of Seasonal Climate Variability on the Salinity in Unsaturated Agricultural Soil. *Agronomy* **2023**, *13*, 2802. https://doi.org/10.3390/agronomy13112802

Academic Editor: Xian Xue

Received: 22 October 2023
Revised: 4 November 2023
Accepted: 6 November 2023
Published: 13 November 2023

Copyright: © 2023 by the authors. Licensee MDPI, Basel, Switzerland. This article is an open access article distributed under the terms and conditions of the Creative Commons Attribution (CC BY) license (https://creativecommons.org/licenses/by/4.0/).

1. Introduction

Agricultural development is directly linked to the level of salinity in the soil as the plant grows better in soils with zero or minimum salt content, leading to high crop fertilization and yield. Indeed, the presence of salt strongly affects plant growth, crop yield, and fertilization [1–3]. However, soils in coastal areas are subjected to severe salt accumulation due to the high salinity of seawater [4–6] and this restrains agriculture development. Reclamation has been used as a process for improving cropland and correcting the salinity situation in coastal areas. The information on climate seasonal variables on salinity distribution is essential to define irrigation schedules and the establishment of guidelines on salt leaching requirements in coastal reclamation areas. Therefore, it is necessary to understand how soil salinity responds to the climate condition at the soil–atmospheric interface and soil salinity distribution in the unsaturated zone in coastal agricultural areas.

The knowledge about salt transportation in the unsaturated zone under climate conditions is of great interest in irrigation and drainage strategies, soil degradation characterization, nutrient management, and water management in natural areas. In some salt-impacted irrigation areas, natural rainfall produces effective leaching under managed water table conditions [7]. Evaporation from saline soils creates salt accumulation near the surface, which subsequently leads to the degradation of soil quality [8,9]. Yan et al. (2015) [10] reported that the climate conditions, groundwater level, and salinity were related to seasonal variability, and there was an increase in groundwater salinity during the dry season. However, the natural processes of salt accumulation and leaching were a combination process due to climate changes [11]. The combined effects of seasonal climate, groundwater level, vegetation, and human activities may result in different results on the spatial and temporal variations of soil salinity among soil profiles [3,10,12]. Additionally, climate variability often results in insufficient leaching in some years, irrigation and drainage management are still needed for leaching soil and controlling salinity [7]. Thus, seasonal climate variability impact on root zone salinity, solute movement at different depths, and the impact on soil properties under various agroecological regions of the world need immediate research attention using hydro-salinity modeling approaches [2].

Many studies have illustrated the soil salinity distribution under evaporation using experimental methods and numerical modeling. Ref. [13] revealed that evaporation at the surface resulted in an upward flow pattern from groundwater, which leads to the formation of high-salt plumes below the evaporation zone. A numerical model developed by Zhang et al. (2014) [14] confirmed that salt precipitates exclusively as efflorescence when there is a hydraulic connection between the surface and groundwater; otherwise, the salt precipitates as sub fluorescence which is the crystallization within the soil pores under the surface layer. Although there are many commercial programs (for example, SWAP and HYDRUS) that have used Richard's equation and the advective–dispersive equation, with a solid physical basis to simulate unsaturated soil water flow and solute transport [15]. These calculations require several input data such as model calibration constants and numerical parameters, and a very fine discretization of space and time [16]. In addition, some models simplify the climate conditions into rainfall and evaporation for calculation by ignoring the complexity of climate conditions. Program Code Bright [17] is able to model the thermo-hydro-mechanical–chemical processes in a coupled way in porous geological media. It can simulate soil–atmosphere interaction by applying boundary conditions simulating rainfall, relative humidity, temperature, wind speed, and radiation, considering at the same time how soil permeability changes with changes in its degree of saturation. This model provided a new insight for us to evaluate the spatial and temporal distribution of unsaturated soil salinity under the condition of seasonal climate variability.

The novelty of this study is to evaluate fundamental knowledge of the solute flux in the vadose zone by advection, diffusion, and dispersion under rainfall and evaporation. And to include a whole climate condition in the finite element simulation under fresh and saline groundwater which is not considered in many other simulations. The objectives of this simulation were to (1) simulate the soil salinity distribution along depth in the unsaturated soil under rainfall, evaporation, and typical seasonal climate variability; (2) evaluate the impact seasonal climate variability has had on soil salinity development in the unsaturated zone; and (3) discuss the dynamics of water flux, solute flux, and salt concentration in the unsaturated zone due to seasonal climate variability.

2. Experimental Site

The soil used in this study is a silty loam collected from the Tiaozini reclamation area (32°50′ N, 120°56′ E) in Jiangsu Province, Eastern China, a region with a semi-humid tropical climate. This reclamation area was established in 2012, when water conservancy measures, drainage, and irrigation systems were built by installing a series of channels for water transport, which would supply fresh water to the soil. The water in these channels would be in close contact with underground water.

The typical mean soil salinity in the studied coastal reclamation areas was appropriately 0.008 kg/kg, which was the initial salinity in the model [18–20] and will increase at the soil surface because of the soil–climate interaction. A schematic section showing the typical cropland is presented in Figure 1, where a fixed water table depth (4 m) is installed. The materials at the zone selected can be considered to be homogeneous and isotropic both from a hydraulic and mechanical point of view. At the vadose zone the in situ average void ratio is 0.827. At the surface, the average annual water content is around 22%, corresponding to a degree of saturation of 74.5% and suction of 0.05 MPa.

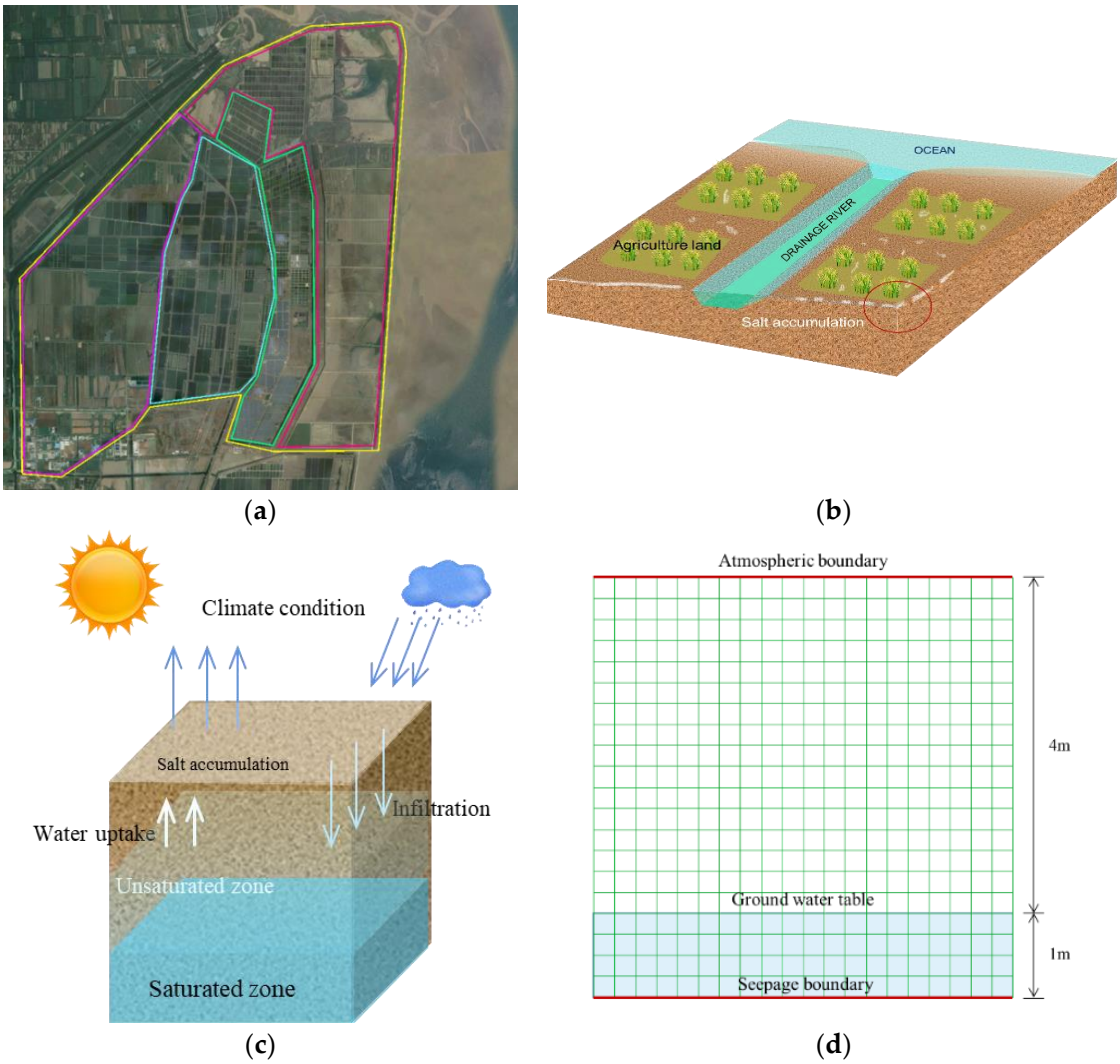


Figure 1. Investigated case: (**a**) map of the Tiaozini reclamation region, different color circles represent different years of reclamation, from left to right represent 1997, 2005, 2008, 2012; (**b**) diagram of the typical coastal reclamation solution; (**c**) scheme illustrating cropland subjected to climate conditions; (**d**) FE mesh adopted.

For the present study, the soil water retention curve (SWRC) was measured using the pressure plate apparatus and adjusted using the expression proposed by van Genuchten [21].

$$\theta_e = \frac{\theta_l - \theta_{rl}}{\theta_{ls} - \theta_{rl}} = \left(1 + \left(\frac{P_g - P_l}{P_0}\right)^{\frac{1}{1-\lambda}}\right)^{-\lambda} \quad (1)$$

where θ_{ls} is the maximum saturation, θ_{rl} is the residual saturation, P_g is the pore air pressure, P_l is the pore water pressure, P_0 is the pressure for a measured temperature, λ is

the shape function. The consistent form of relative permeability with the van Genuchten–Mualem model,

$$k_{rl} = \sqrt{\theta_e}\left(1 - \left(1 - \theta_e^{1/\lambda}\right)^{\lambda}\right)^2 \quad (2)$$

where k_{rl} is the coefficient for liquid relative permeability, λ is a constant. Figure 2 presents the experimental points and the adjustment of the SWRC of the soil. The saturated permeability is 19.8 mm/h, measured using a constant water head apparatus.

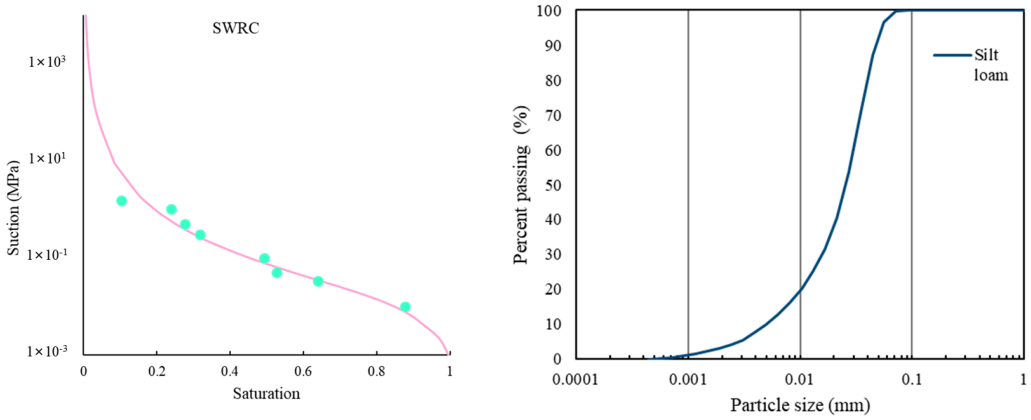


Figure 2. (**a**) Soil water retention curve and (**b**) particle size distribution of the silt loam used in the simulation.

The climate condition in the studied reclamation area is a subtropical monsoon climate. The subtropical monsoon climate is controlled by tropical marine air masses during the summer and polar continental air masses in the winter, resulting in lower temperatures and precipitation in winter, and the opposite in summer. Figure 3 presents the corresponding typical monthly climate data (rainfall, temperature, relative humidity, and wind speed) collected in 2017 from ERA5 monthly averaged data on a single level from 1979 to the present provided by the European Centre for Medium-range Weather Forecasts (ECMWF) [22].

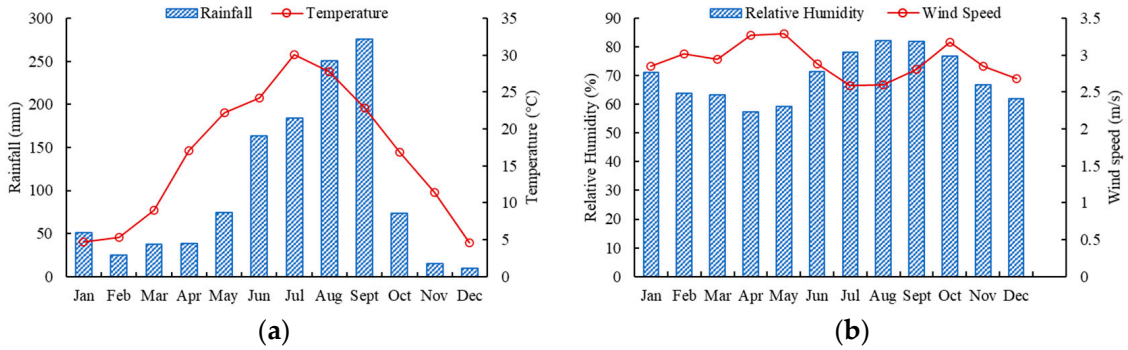


Figure 3. Climate data in one year from Dongtai: (**a**) monthly rainfall and temperature; (**b**) monthly relative humidity and wind speed [22].

3. Method and Model

3.1. Cases Simulated

The salt transport process of the unsaturated soil under the climate condition at the soil–atmospheric interface and the interaction between unsaturated cropland and the atmosphere was modeled using Code_Bright (2022_6).

Three climate conditions and two groundwater salinity were simulated in this study. Case 1 considered only rainfall without evaporation to simulate the salt leaching process

(considering only fresh groundwater), and Cases 2 and 3 simulated the salinization process due to evaporation without rainfall, under fresh and saline groundwater supplement from the underground water table, respectively. It was important to consider both fresh and salty water to mimic in situ conditions, as water in the channels is fresh upstream but becomes salty along the channel if the desalinization system is working properly. The complete atmospheric boundary conditions were applied in Cases 4 and 5 using the climate data previously presented in Figure 3, based on Cases 2 and 3, respectively. The simulation of these cases was carried out for 1 year, recording the results for every 5 days.

A final study considering a 5-year simulation was performed based on Cases 4 and 5, in which the average annual climate was repeated. The idea of a 5-year simulation was to investigate whether soil salinity is suitable for planting crops under natural climate conditions after a 5-year simulation, or whether further soil salt leaching methods should be taken because reclamation needs to plant crops and produce benefits as soon as possible. This study allowed us to understand how soil salinity would change over time under current climate conditions and desalinization solutions adopted in the Tiaozini reclamation area.

3.2. FE Model and Initial Conditions

A vertical section of the site (with dimensions 5 m by 5 m) was adopted to represent the homogeneous soil, being divided into quadrilateral finite elements with a 25 cm mesh size (400 elements and 441 nodes in total, see Figure 1d). Climate conditions, which include rainfall, relative humidity, temperature, atmospheric pressure, and wind speed, were applied as boundary conditions at the top of the soil layer.

The soil saturation profile adopted for the different depths is presented in Figure 4. Suction was assumed to increase linearly from zero, at the water table depth, until the surface where it was 0.05 MPa. This corresponds to the degree of saturation of 74.5% for this soil at the surface, defined considering experimental data. The initial salt concentration in the soil was 0.008 kg/kg which is measured in situ.

Flooding freshwater irrigation and pipe drainage methods have been used to transport fresh water and facilitate soil desalinization in coastal reclamation areas [20]. However, Yan et al. (2015) [10] reported that the groundwater level in the coastal plain of Eastern China was shallow and easily affected by precipitation and evaporation. The model with a fixed water table had a stable hydraulic connection between the surface layer and water table [23], which would reduce the complicity of the numerical model and focus more attention on the salt transport processes due to precipitation and evaporation. Additionally, the water table depth can be maintained at the appropriate level by engineered drainage systems to achieve favorable conditions for crop growth [7,24]. The model assumed that the extra water due to precipitation would drain fast from the bottom by the drainage channel and water loss due to evaporation is compensated by water transported from the water table. Since leaching the salt downward through the root zone with additional irrigation water was widely used to control the soil salinization. Whether additional fresh groundwater is needed to facilitate salt leaching from the bottom has not been investigated. The groundwater table was controlled at 4 m to represent shallow groundwater recharge, intending to mimic an in situ desalinization system. Two supply groundwater salinity levels were considered, corresponding to freshwater (Cases 1, 2, and 4) and saltwater (Cases 3 and 5). They allowed us to understand (i) salt leaching by rainfall (Case 1); (ii) the effect of evaporation on soil salinization (Cases 2 and 3); and (iii) the effect of climate actions on soil salinity distribution (Cases 4 and 5). Table 1 summarizes the cases studied. This table also includes the constants for the model, namely temperature (T), atmospheric gas pressure (Pg), relative humidity (RH), average annual precipitation in the region (P), average wind speed (v_a), and groundwater salinity.

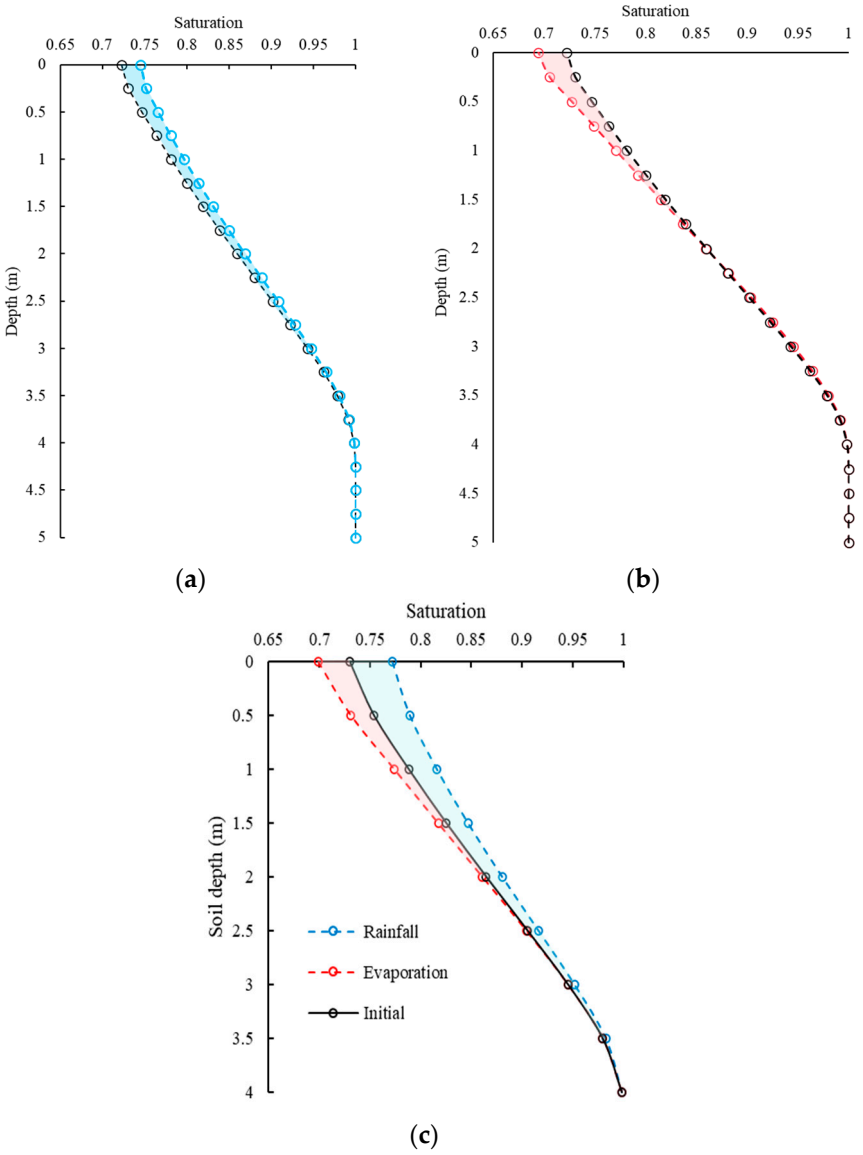


Figure 4. Degree of saturation at different depths: (**a**) rainfall, (**b**) evaporation, (**c**) climate action before and after the simulation.

Table 1. Cases studied, initial conditions, and fixed climate data.

Parameters	Case 1 (Rainfall)	Cases 2 and 3 (Evaporation)		Cases 4 and 5 (Climate)	
T (°C)	25	25		Climate data See Figure 3	
P_{ga} (MPa)	0.1	0.1			
HR (%)	68%	68%			
P (mm)	1010	0			
v_a (m/s)	3.15	3.15			
Groundwater salinity (kg/kg)	0	0	0.008	0	0.008

Note: T is atmospheric temperature; P_{ga} is atmospheric gas pressure; HR is relative humidity; P is rainfall; v_a is wind velocity.

3.3. Simulation of Salt Transport

The problems solved by Code_Bright consider the phases solid (-), liquid (l), and gas (g), and the species solid (-), water (w), air (a), salt (s), and vapor (v). The equations to be solved when computing solute migration (NaCl) in the soil under seasonal climate, neglecting soil volume changes, are mainly those corresponding to the transport of water

(both in liquid and gas phases, by advection and diffusion), solute (advection, diffusion, and dispersion) and energy (conduction). The summary of the soil parameters and constitutive laws related to these problems are provided in Table 2, which also presents the calibration constants used.

Table 2. Constitutive laws, material parameters, and values used in the simulation.

Constitutive Laws	Model	Material Parameters	Legend
Liquid advective flux (Darcy law) b	$q_l = -\left(\frac{kk_{rl}}{\mu_l}\right)(\nabla P_l - \rho_l g)$	$k = 5.5 \times 10^{-13}$ m^2 $\mu_l = 0.89$ MPa s $\rho_l = 1$ g/cm^3 g = 9.8 m/s^2	q_l: liquid flow k: intrinsic permeability μ_l: liquid viscosity ρ_l: liquid density g: gravity P_l: liquid pressure
Water retention curve [21]	$S_e = \frac{S_l - S_{rl}}{S_{ls} - S_{rl}} = \left(1 + \left(\frac{P_g - P_l}{P_0}\right)^{\frac{1}{1-\lambda}}\right)^{-\lambda}$	$\lambda = 0.3631$ $P_0 = 0.03$ MPa $S_{rl} = 0.017$ $S_{ls} = 1$	S_e: degree of saturation S_{ls}: maximum saturation S_{rl}: residual saturation P_g: gas pressure P_0: pressure for a measured T λ: shape function
Liquid flow	$k_{rl} = \sqrt{S_e}\left(1 - \left(1 - S_e^{1/\lambda}\right)^{\lambda}\right)^2$	$\lambda = 0.3631$	k_{rl}: coefficient for liquid relative permeability λ: constant
Diffusive fluxes of vapor	$D_g^v = D\left(\frac{(273.15+T)^n}{P_g}\right)$	$D = 5.9 \times 10^{-6}$ m^2/s $n = 2.3$ $P_g = 1 \times 10^5$ Pa	D_g^v: diffusion coefficient of vapor in gas phase P_g: gas pressure T: Temperature
Diffusive fluxes of salt	$D_l^s = D\exp\left(\frac{-Q}{R(273.15+T)}\right)$	$D = 2.59 \times 10^{-9}$ m^2/s $Q = 24{,}530$ J/mol	D_l^s: diffusion coefficient of salt in liquid (m^2/s) D: constant Q: constant
Dispersive fluxes of mass [25]	$D_l' = d_l\lvert q_l\rvert \mathrm{I} + (d_l - d_t)\frac{q_l q_l^t}{\lvert q_l\rvert}$	$d_l = 0.5$ m $d_t = 0.05$ m	D_l^l: dispersion coefficient of salt in liquid d_l and d_t: longitudinal and transverse dispersivity for solutes in liquid phase
Conductive flux of heat [26]	$\mathrm{i}_c = -\lambda\nabla T$ $\lambda_{dry} = (1-\phi)^n\lambda_{solid} + \phi^n\lambda_{\mathrm{gas}}$ $\lambda_{sat} = (1-\phi)^n\lambda_{solid} + \phi^n\lambda_{liq}$	$\lambda_{solid} = 2$ W/mK $\lambda_{liq} = 0.6$ W/mK $\lambda_{gas} = 0.024$ W/mK	i_c: conductive heat flux λ: thermal conductivity ϕ: porosity

Darcy's law generalized for the unsaturated case was used for simulating transport by advection. The intrinsic permeability of the soil (k) was constant and defined considering the experimental data available. The coefficients for the relative permeability of liquid and air (k_{rl} and k_{rg}, respectively) were defined as a function of the degree of saturation (θ_e), being the coefficient for the liquid relative permeability computed using the soil water retention defined by van Genuchten equation (Equation (2) and Table 1).

The non-advective flux of a species (i) in phase (α) considers molecular diffusion and mechanical dispersion. Fick's law for molecular diffusion was used to describe the diffusive fluxes of vapor in the gas phase and dissolved salt in the liquid phase:

$$i_\alpha^i = -\left(\tau\phi\rho_\alpha\theta_\alpha D_\alpha^i\right)\nabla\omega_\alpha^i \quad (3)$$

where τ is the coefficient of tortuosity, ϕ is porosity, ρ_α is density, θ_α is degree of saturation, ω_α^i is a mass fraction, D_α^i is the diffusion coefficient of species (i) in phase (α). Only the

vapor (v) species in the gas (g) phase and salt (s) species in the liquid (l) phase were considered (constant parameters in Table 2) due to the absence of data.

The mechanical dispersion mass flux was calculated using Fick's law equation to describe dispersity for vapor, dissolved air, and slat:

$$i_\alpha^i = -\left(\rho_\alpha D'_\alpha\right)\nabla\omega_\alpha^i \tag{4}$$

where D'_α is the mechanical dispersion tensor defined in Table 1.

Thermal conductivity is used in Fourier's law to compute conductive heat flux:

$$i_c = -\lambda\nabla T \tag{5}$$

The conductivity of the phases of the soil is given in Table 1.

The leaching rate was introduced to describe the efficiency of salt leaching, which can be defined as the ratio of the concentration reduction per day:

$$L_r = \frac{C_i - C_{i+5}}{5} \tag{6}$$

where C_i is the salt concentration at i (i = 0, 5, 10. . .) days (kg), C_{i+5} is the salt concentration at i + 5 days (kg), L_r is the salt leaching rate (kg/(kg·day)), positive value means leaching while negative value means accumulating.

3.4. Climate Boundary Condition

Climate data is considered in Code_Bright by the subroutine of atmospheric boundary condition, which first reads the atmospheric data from the file and then computes water flux, air flux, and energy flux. The equations for calculating the fluxes are described.

The advective flux of air is considered as:

$$j_a = \omega_g^a q_g = \left(1 - \omega_g^w\right) q_g \tag{7}$$

where j_a is the flux of air, ω_g^a is a prescribed mass fraction.

The evaporation water flux was calculated based on the aerodynamic diffusion relation:

$$E = \frac{k^2 v_a \varphi}{\left(\ln\frac{z_a}{z_0}\right)^2}(\rho_{va} - \rho_v) \tag{8}$$

where k is von Karman's constant (0.4), v_a is the wind velocity, φ is the stability factor (1.0), z_a is the screen height (2 m) at which v_a and ρ_{va} were measured, z_0 is the roughness length which is (0.02 m) to represent 10–50 cm high grass surface, ρ_{va} is the absolute humidity of the atmosphere at the screen height and ρ_v is the absolute humidity at the soil surface.

The advective flux of vapor by the gas phase j_g^w is written as:

$$j_g^w = \omega_g^w q_g \text{ if } P_g > P_{ga} \tag{9}$$

$$j_g^w = \frac{\rho_{va}}{\rho_{ga}} q_g \text{ if } P_g \le P_{ga} \tag{10}$$

where ρ_{ga} is the atmospheric gas density and q_g is the flux of the gas phase given by Equation (4).

Surface runoff is considered as follows:

$$j_{sr} = \gamma_w\left(P_l - P_{ga}\right) \text{ if } P_l > P_{ga} \tag{11}$$

$$j_{sr} = 0 \text{ if } P_l \le P_{ga} \tag{12}$$

where γ_w is the leakage coefficient of water. If the soil is saturated ($P_l > P_{ga}$) all rainfall that cannot infiltrate will runoff. Surface runoff corresponds to the flow rate of water through the liquid phase j_l^w.

The total water flux is the sum of rainfall P, evaporation E, and advective flux of the vapor gas phase j_g^w and of surface runoff.

$$j_w = k_{rain}P + k_{evap}E + j_g^w + j_{sr} \quad (13)$$

where k_{rain} and k_{evap} are the coefficients of rainfall and evaporation (default values equal to 1 were adopted).

4. Results

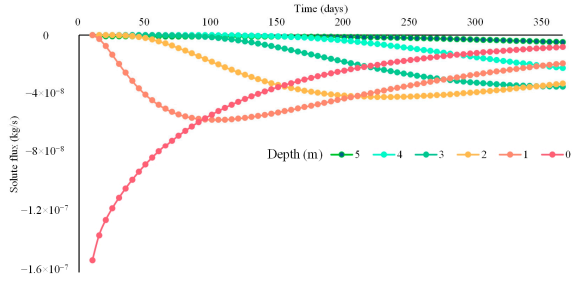
4.1. Understanding Salt Transport Caused by Rain and Evaporation

4.1.1. Salt Leaching by Rainfall

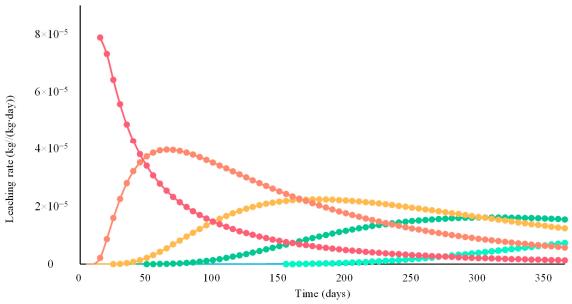
The results of salinity distribution after rainfall infiltration allowed us to understand better the salt leaching process in the vadose zone (Case 1). The seepage boundary condition at the base allowed (fresh) water to flow in and out, and the water table was fixed; therefore, the degree of saturation did not change significantly (increased from 72% to 75% at the surface, see Figure 4a) and salt concentration changed mainly due to diffusion and dispersion in the liquid phase. This is interpreted from now on as salt leaching. The solute flux by diffusion and dispersion decreased over time (see Figure 5a). At the end of the year, the salt concentration decreased from the initial value of 0.008 kg/kg to 0.0002 kg/kg at the soil surface, while at the depth of the water table, this initial concentration only decreased to 0.0067 kg/kg.

Leaching caused by water infiltration towards the base explains the decrease in salt concentration over time in the entire depth (see Figure 6). The reduction of soil salinity observed above the water table was much higher and faster than that found for the deeper soil, and the distribution of salt concentration presents a nonlinear profile through all time instants.

The leaching rate above 1 m depth decreased significantly over time and salinity became approximately constant in this upper layer when the values reached were almost null at the soil surface (Figure 5b). The leaching rate under the water table increased with time, but was much lower than that found in the upper part (Figure 5b). The results confirm that the salt leaching rate in the unsaturated soil profile varies nonlinearly with time, which is associated with infiltration rate, salt concentration or with the unsaturated liquid phase permeability related to changes in the degree of saturation.



(**a**) Solute flux under Case 1



(**b**) Leaching rate under Case 1

Figure 5. *Cont.*

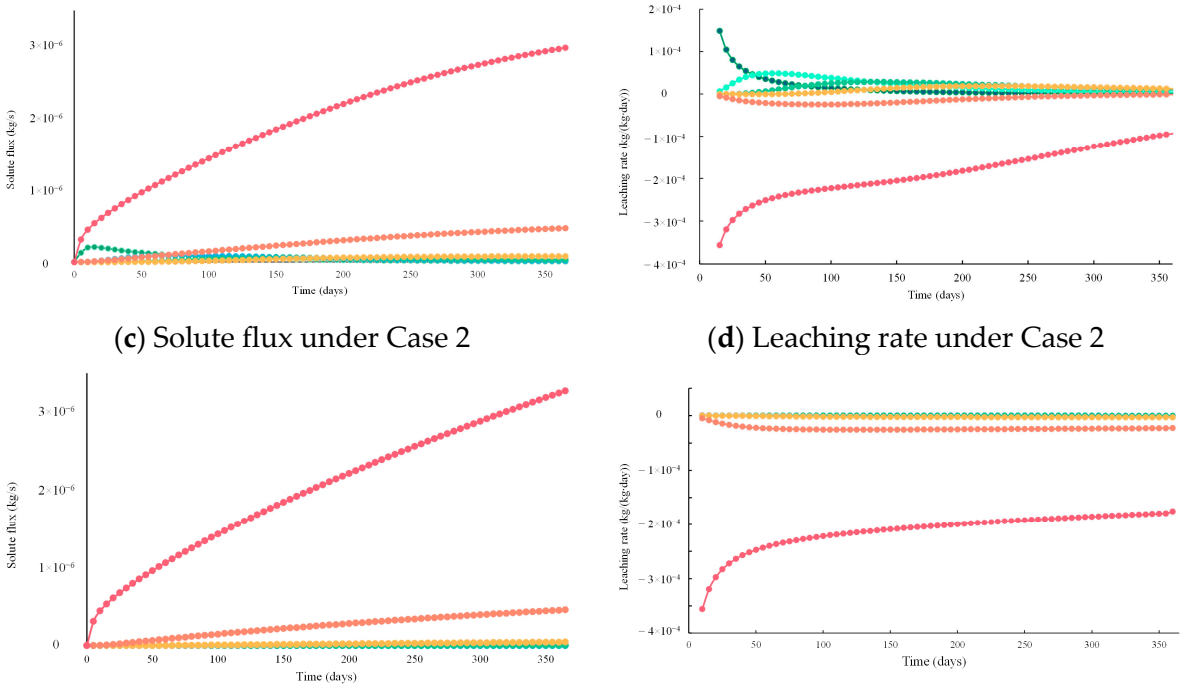


Figure 5. Simulated solute flux (by diffusion and dispersion) under (**a**) rainfall and (**c**,**e**) evaporation events. Leaching rate under (**b**) rainfall and (**d**,**f**) evaporation. Negative solute flux means the direction was upwards and a positive value means downwards. A positive leaching rate means leaching while negative means accumulating.

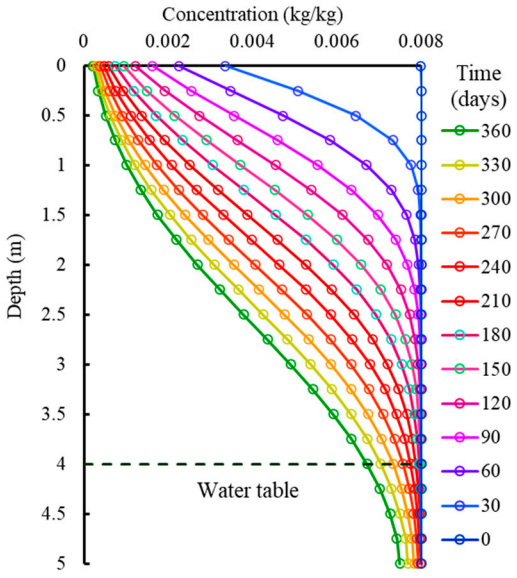


Figure 6. Evolution of salt concentration at different depths due to rainfall with a fixed water table (Case 1).

4.1.2. Salt Accumulation by Evaporation

Two different salinities of groundwater (fresh groundwater and salt concentration of 0.008 kg/kg, respectively, for Cases 2 and 3; see Table 2) were considered to compute the salinity distribution under evaporation in the 1-year simulation. The degree of saturation and water content of the soil did not significantly change during evaporation (decreased from 72% to 70%; see Figure 4b) because underground water was supplied. As presented

in Figure 5c,e, the solute flux by diffusion and dispersion significantly increased with time at different depths. The accumulation rate at the surface and beneath the water table both decreased over time under fresh groundwater, while the leaching rate beneath the water table remained constant for saline groundwater conditions (Figure 5d,f). Salt accumulation processes of these two groundwater salinity conditions for the soil layers above 1.5 m depth were similar for both water sources (Figure 7). The salinity at the surface increased from 0.008 kg/kg to 0.088 kg/kg and 0.079 kg/kg for the saline and fresh groundwater supplements, respectively. This increment was expected because the water was moving upwards in the soil layer by advection and vapor diffusion, and evaporated from the ground surface, carrying salt by advection, which also could diffuse through the liquid phase.

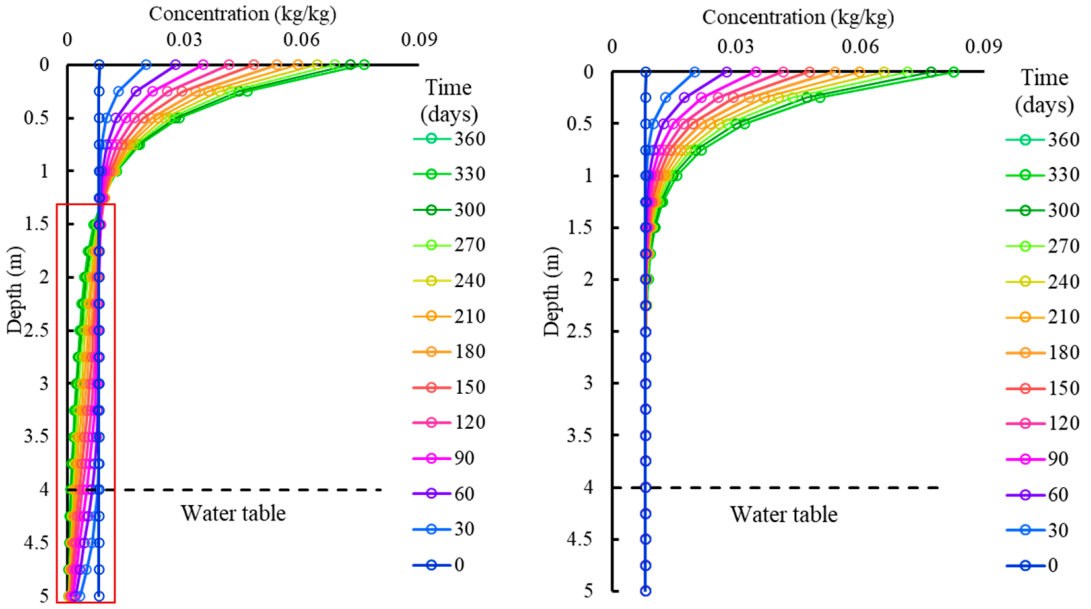


Figure 7. Evolution of salt concentration due to evaporation with a fixed water table supplied with (**a**) fresh (Case 2) and (**b**) saline (Case 3) groundwater. Red frame represent the differences between Case 2 and Case 3.

The salt concentration distribution below 2 m depth was constant when saline groundwater was supplied, while its concentration decreased with increasing time for the case of freshwater supply. This is the desalinization expected when fresh water was supplied, which was successful because salinity tended to reach 0 below groundwater level after 1 year.

The soil saturation distribution below 2 m was not significantly changed at different times (see Figure 4b) and the degree of saturation is around 85%. This degree of saturation is close to that of the air entry value (see the water retention curve of the soil, Figure 2) which indicates that the liquid phase was continuous and therefore both salt diffusion and dispersion through the liquid phase could occur.

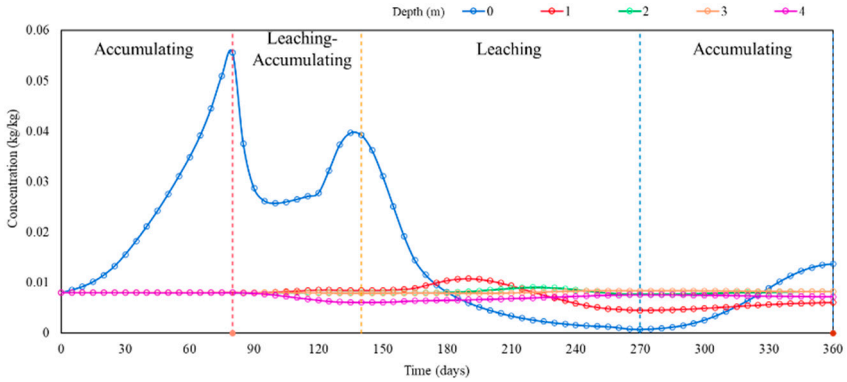
This equilibrium saturation distribution provided a constant water flux by liquid advection to explore a clear diffusion and dispersion mechanism of salt transport in the vadose zone with a stabilized saturation [27,28]. The simulations explained the solute movements under rainfall and evaporation at different depths in unsaturated conditions and provided fundamental knowledge in modeling climate effects on soil salt distribution.

4.2. Effect of Climate Action on Salinity Distribution

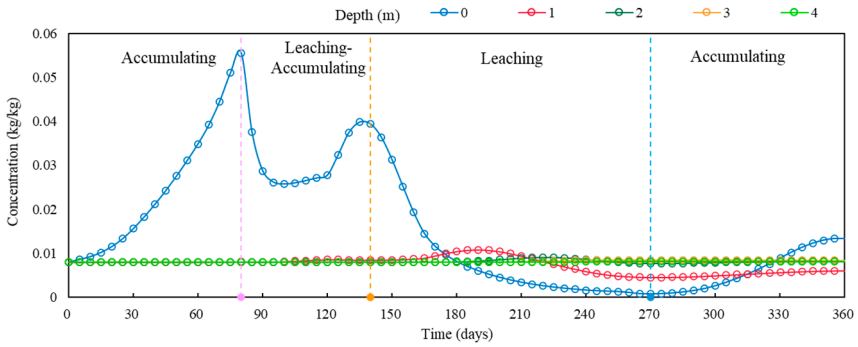
4.2.1. One-Year Simulation

After simulating the rainfall and evaporation on soil salt concentration distribution separately, the effect of real climate action on soil salt concentration distribution was investigated. The annual climate data (Figure 3) was used in the first study, and then the same climate conditions were repeated for 5 years to evaluate the salt leaching efficiency by natural seasonal climate conditions.

The response of unsaturated soil saturation to the soil–atmosphere interface affected the soil salt distribution significantly. As presented in Figure 8, the soil salt concentration distribution near the soil–atmospheric interface was significantly influenced by seasonal climate variability. The concentration varied dynamically depending on drying and rainy seasons, now considering infiltration and evaporation also caused by temperature and wind, not only by rain and relative humidity.



(**a**) Fresh groundwater (Case 4)



(**b**) Saline groundwater (Case 5)

Figure 8. Variations of the salt concentration in the unsaturated soil zone at different depths with fresh groundwater supply (**a**) and saline groundwater supply (**b**). Results from 1-year simulation.

As found in the results of Cases 2 and 3, the salt concentration varies in depth, and over time, being these changes more marked at the surface and mainly until 2 m depth [29]. These results were similar for both groundwater salinities. The changes found below 4 m depth were stable over time for the saline groundwater supply, indicating desalinization in the case of freshwater.

According to the salt concentration distribution at the vadose zone, the salt distribution dynamically caused by climate action could be divided into four processes (Figure 8): (1) salt accumulation during winter, which is a dry and cold season (days 0–80); (2) salt leaching and slightly accumulation during spring (days 80–140); (3) salt leaching during summer, which is a wet and hot season (days 140–270); (4) salt re-accumulation during autumn (days 270–365).

For the first salt accumulation process (days 0–80), the salt transport was like the one found when the evaporation process was simulated. The salt concentration at the

surface was accumulated from 0.008 to 0.055 kg/kg (Figure 8a). In the following days, salt leaching occurred and salt concentration at the surface reduced from 0.055 to 0.032 kg/kg (day 80–120); however, there was an increment in salt concentration at 1 m depth, presenting a small peak. This indicates that fresh water from rain infiltration has not reached this depth yet and salt transport by diffusion is prevailing. Evaporation continues while the temperature is rising but rain is still not intense and for this reason, salt concentration on the surface increases to 0.039 kg/kg (day 120–140). This transition period gives place to a clear raining period (days 140–270), where infiltration prevails and the leaching process continues in the entire depth of the vadose zone. Salt concentration will reduce until almost zero (0.00074 kg/kg) at the surface, directly in contact with clean water from rain, and will move downward with water (transport by advection and dispersion) in the unsaturated zone (Figure 9). The salt concentration in the vadose zone no longer presents a peak (Figures 9c and 10c). At this period, the groundwater salinity has a limited influence on the salt concentration in the vadose zone. The salt concentration at the surface increases when the dry season comes again (day 270–365) and can reach 0.014 kg/kg at 360 days (Figures 9d and 10d). This result is in accordance with field observations in salted soils in which salt concentrates closer to the surface form a whitish layer [30].

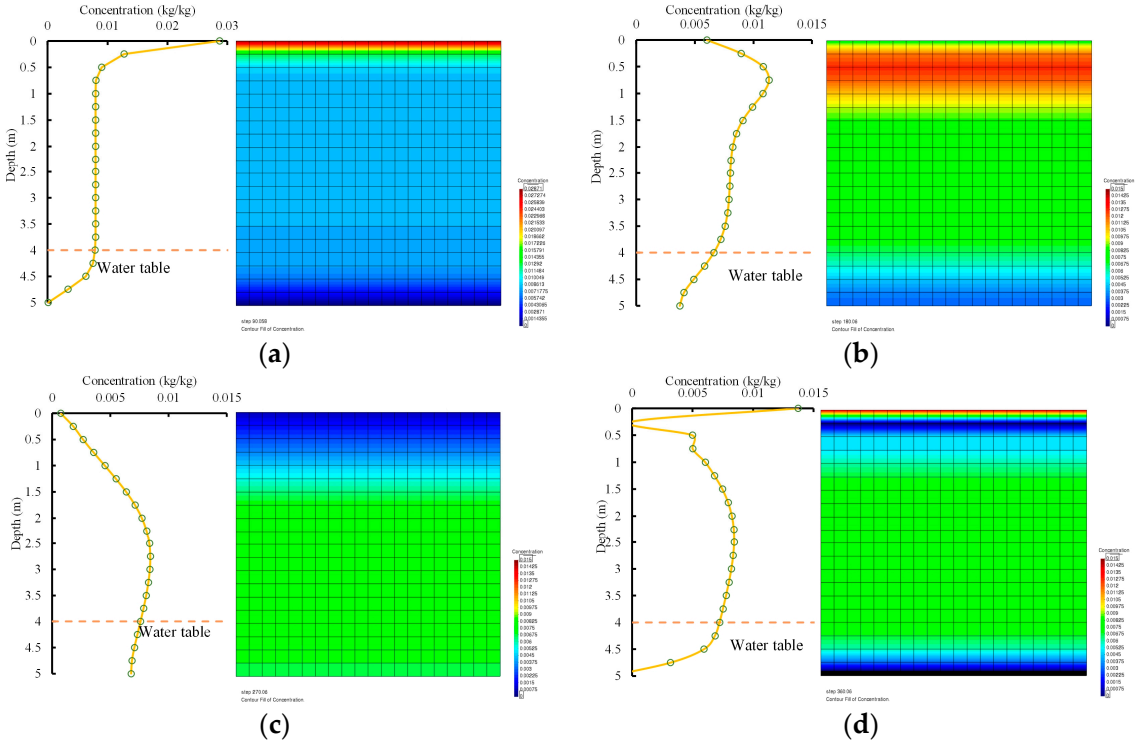


Figure 9. Soil salt concentration distribution at (**a**) 90 days, (**b**) 180 days, (**c**) 270 days, (**d**) 360 days with fresh groundwater supply (Case 4). The left-hand graph is the salt concentration distribution at different depths. The right hand is the contour fill of salt concentration. (**b**–**d**) has a smaller scale than (**a**) to clarify significant differences for corresponding intervals.

The changes reported are also presented in Figure 11. It is also noticeable that, during one year of simulation, soil salt concentration at 2 m to 3.5 m depth has not changed much with climate action and always remained with the initial concentration. Below ground water, the differences found between fresh and saline groundwater supplies were similar to those observed under evaporation conditions, which are that salinity reduces over time in the presence of fresh water, and remains constant when water is saline (Figure 11).

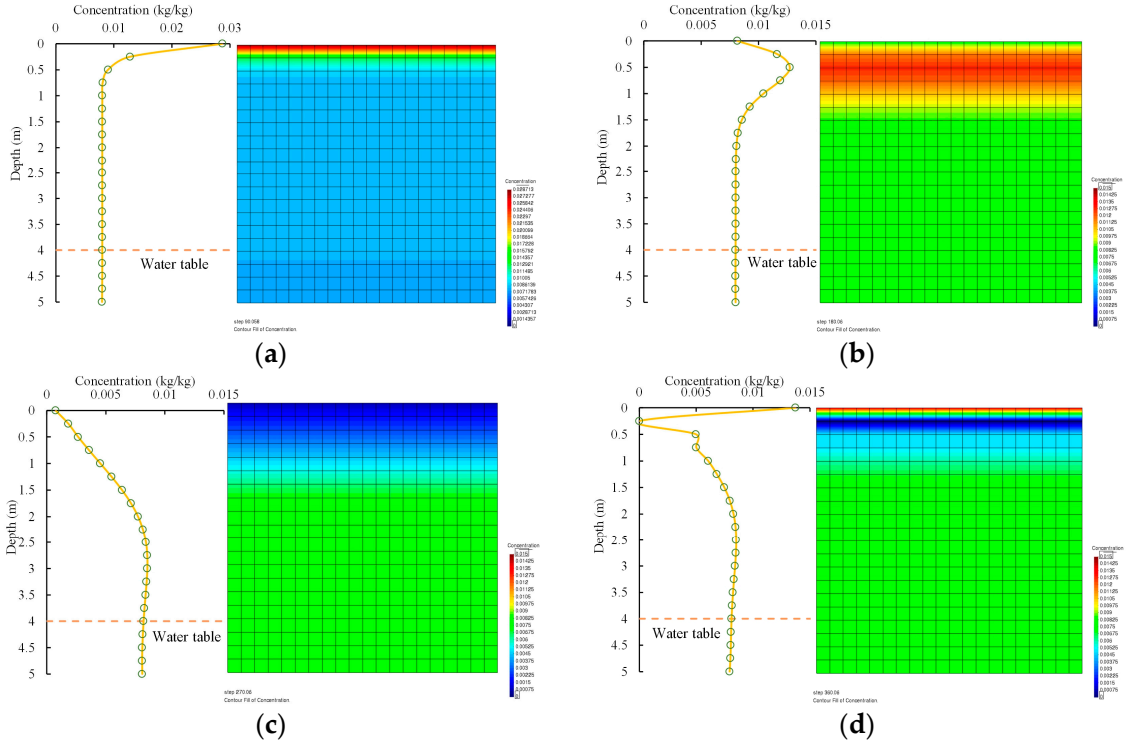


Figure 10. Soil salt concentration distribution at (**a**) 90 days, (**b**) 180 days, (**c**) 270 days, (**d**) 360 days with saline groundwater supply (Case 5). The left-hand graph is the salt concentration distribution at different depths. The right hand is the contour fill of salt concentration. (**b**–**d**) has a smaller scale than (**a**) to clarify significant differences for corresponding intervals.

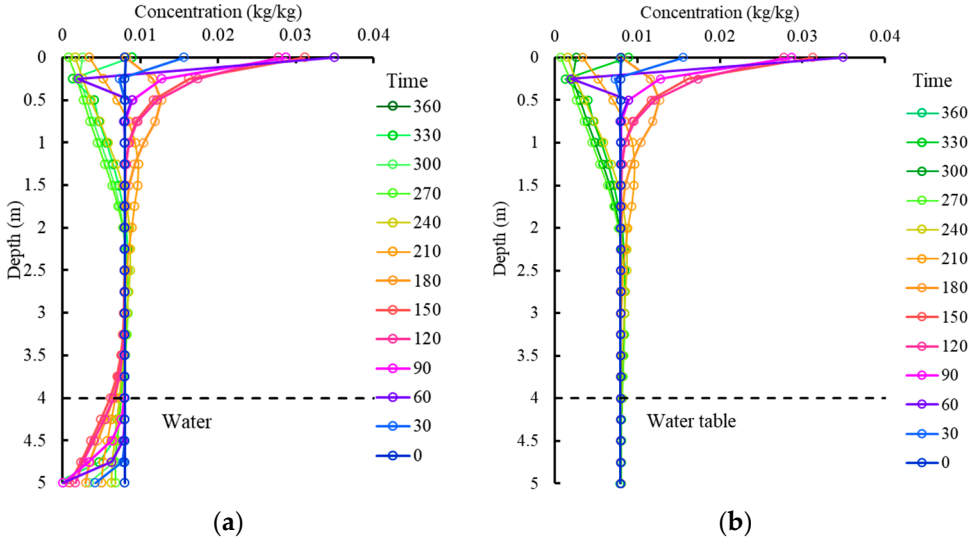
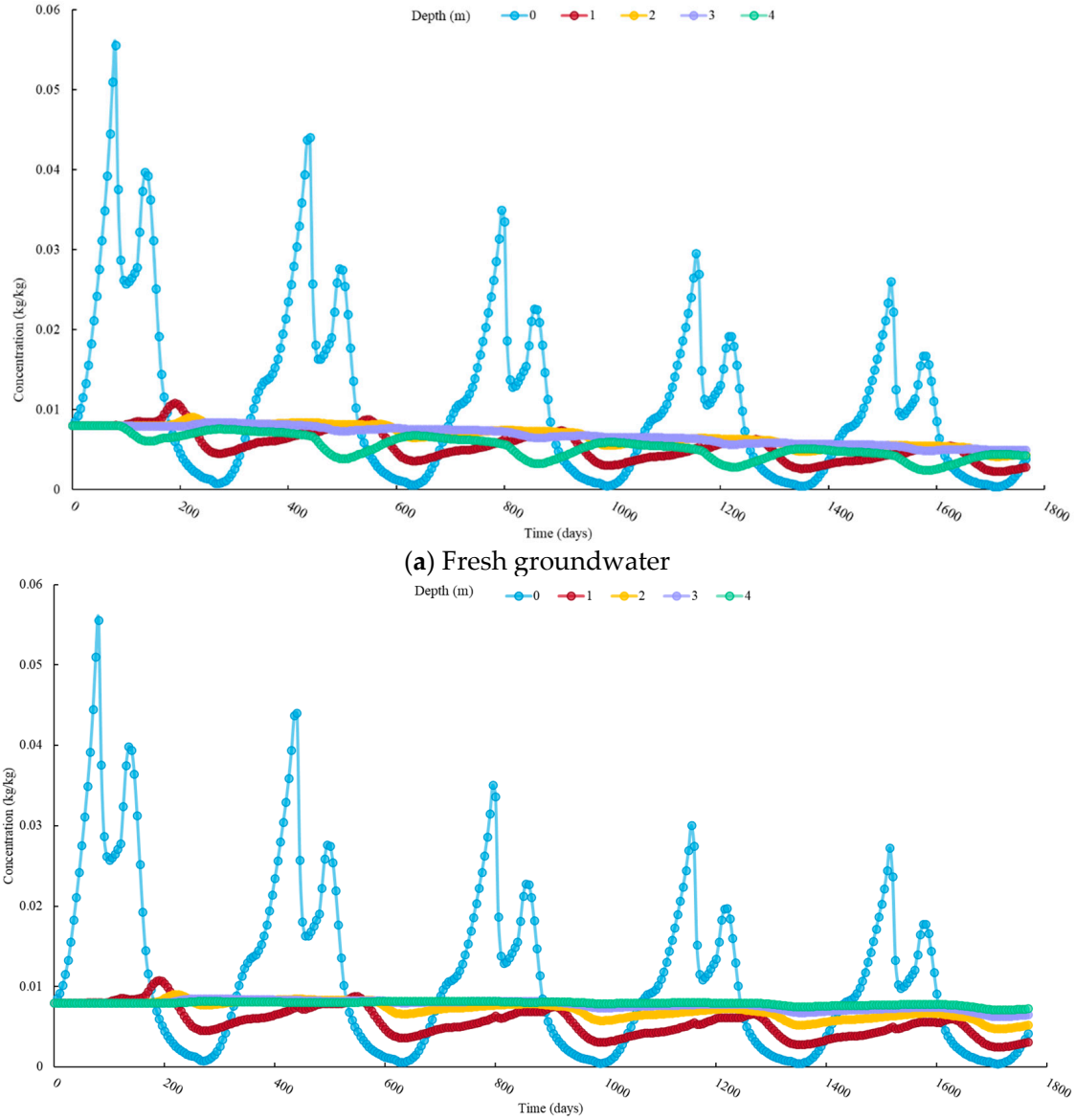


Figure 11. Simulated history results of salt concentration at different depths with (**a**) fresh groundwater supply (Case 4); (**b**) saline groundwater supply (Case 5).

4.2.2. Study for 5 Years

The same average annual climate data was repeated for 5 years keeping the water table fixed at 4 m and allowing the free flow of fresh water. In this manner, the groundwater could rapidly recover. The time evolution of the salt concentration in different depths of the vadose zone (surface, 1, 2, 3, and 4 m depths) is presented in Figure 12. As expected, the path observed for the one-year simulation (Figure 8) is repeated in the following years; however, with a progressive reduction in the maximum values found in the following

years (0.055, 0.044, 0.033, 0.029, and 0.026 kg/kg at years 1, 2, 3, 4 and 5, respectively). This indicated that salt leached faster for the first three years and became slower when the concentration decreased. However, at the vadose zone, the salt concentration beneath 1 m did not decrease as much as that in the surface and the oscillation values are similar for the 5 years. The salinity below the groundwater level decreased with time under fresh groundwater supply.



(**a**) Fresh groundwater

(**b**) Saline groundwater

Figure 12. History results of salt concentration in the unsaturated zone under 5-year simulation with fresh groundwater (**a**) and saline groundwater (**b**) supply.

The degree of saturation of the soil at different depths (Figure 13) has changed in accordance with climate, increasing in the rainy seasons and decreasing in the dry ones. However, the values at the surface varied little, from 0.7 to 0.77, which probably explains the fact that salt leaching was not very marked for the climate exposition in the 5 years. These results indicate that the salt concentration in the cropland remains high and has a strong potential to seriously affect agricultural production after 5 years of natural climate leaching.

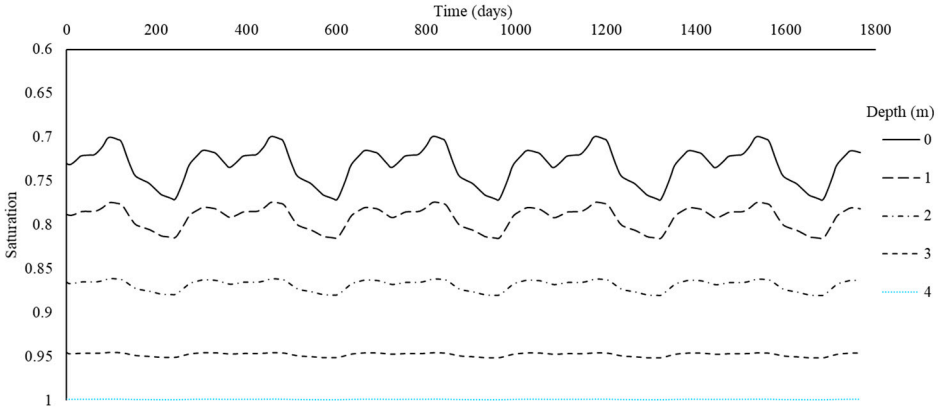


Figure 13. History results of soil saturation at different depths in the vadose zone along 5-year simulation.

5. Discussion

The soil salinity distributions in the unsaturated soil under rainfall and evaporation were computed by the finite element model. This model simulated the salt leaching process during rainfall and the salt accumulation process during evaporation.

In rainfall events, fresh water from rain has infiltrated and salt leached downward to groundwater [28,31]. However, the soil salinity reduced nonlinearly in the unsaturated zone because the degree of saturation did not change significantly and was below the one corresponding to the air entry value of the soil at the surface layers. This may indicate that salt transport by dispersion in the liquid phase is interrupted and only diffusion takes place. For instance, diffusion may become more important if the advection is small. Due to the constant saturation along the depth, the liquid advection was constant, but the leaching rate decreased at the surface (Figure 5b). This is because the salt concentration at the surface changes significantly (Figure 6), which results in diffusion and dispersion decreasing at the surface and increasing at the deeper layer (Figure 5a). Such differences in diffusion and dispersion at different depths would bring salt at deeper layers to the surface, thus reducing the leaching rate. As soil salt concentration decreased from the surface under rainfall infiltration, the solute diffusion and dispersion at the surface by rainfall would reduce and more time was needed for the freshwater to move down to the targeted leaching soil depth.

According to the simulation under evaporation with a fixed saline/fresh water table, the results of the soil salinity distribution demonstrated a significant salt accumulation process at the surface. This is because only the water evaporates from salty water, and water vapor is migrating from depth, increasing salt concentration in the shallow soil surface layers. This accumulation was caused by evaporation-induced water uptake and upward capillary flow. As salt in the liquid phase increased with water flow by liquid advection, the concentration increased at the surface resulting in the significant increment of downward solute flux by diffusion and dispersion; thus, the salt accumulates slower over time (Figure 5d,f). In the present work, the water evaporated was supplied by groundwater to maintain the equilibrium moisture condition at the soil surface. Therefore, only a transition zone and lower region with water flow existed and the model was not able to simulate the appearance of a salt crust. However, the model was able to simulate the accumulation of salt near the surface (between 0 and 1 m depth), suggesting the formation of this crust.

Climate actions had a significant effect on the rearrangement of salinity distributions in the unsaturated zone under fresh/saline groundwater [32]. According to the results of the simulation for 5 years, the unsaturated soil experienced salt accumulation in dry seasons and leaching in the wet ones. This is closely related to seasonal precipitation and climate variability. In the simulation of the climate effects on salinity distribution, the soils were also subjected to wetting–drying cycles when the season changed, mostly when entering

the rainy season. The dynamics of salt distribution in the vadose zone (between 1 and 4 m depth) maintained its initial value (Figure 11). Due to the soil water content, the soil salinity response to climate variability significantly at the surface–atmospheric interface, while the soil salinity below the surface was insensitive to the climate condition (Figure 12). In general, the numerical results found that the climate action with fresh underground water supply had a low impact in reducing salt concentration at the end of 5 years, indicating low efficiency in the salt leaching process, especially when the water in the drainage channel becomes salty during drainage. This would enhance the diffusion and dispersion of salt in the liquid phase, thus reducing the leaching rate, according to the simulation on rainfall and evaporation. Due to the low salinity tolerance of rice, such high-level salinity at the soil surface after simulation would restrict the development of agriculture [33].

The results were also important to know the soil salt content distribution at the vadose zone. The results found that soil salinity near the soil surface (0–50 cm) was easily changed due to climate action. The soil salt content decreased during the wet season, while increasing during the dry season. The soil salt content in the deeper vadose zone was hard to leach and would affect the soil leaching efficiency in the vadose zone by diffusion and dispersion. Additional fresh groundwater supplement from the bottom would have a significant leaching efficiency than that of saline groundwater.

6. Conclusions

It has been investigated that the seasonal climate condition at the soil–atmospheric interface plays an essential role in the salinity distribution and solute transport in the unsaturated zone. This study conducted a finite element numerical analysis to explore the soil salinity response to climate conditions at the soil–atmospheric interface. The conclusions are as follows:

(1) Rainfall at the surface induced a downward flow pattern in the unsaturated zone that led to a salt leaching process with nonlinear efficiency. Due to evaporation, the water moves upwards transporting salt to the surface, and therefore the soil salinity above the evaporation front can be remarkably higher. The significant change in salt concentration under rainfall and evaporation would enhance the salt diffusion and dispersion, thus reducing leaching/accumulating efficiency. The soil salinity beneath the evaporation front remained steady with saline groundwater and decreased with evaporation with fresh groundwater.

(2) The seasonal climate had a significant effect on the soil salinity redistribution in the vadose zone. The model can compute the salt accumulation process during the dry season and the salt leaching process during the wet season. Salt decreased fast for the first three years (i.e., the highest value decreased from 0.055 to 0.033 kg/kg), but decreased slower for the last two years (i.e., the highest value decreased from 0.033 to 0.026 kg/kg). The salt leaching efficiency decreased with time under natural climate action. Fresh groundwater supplements would be helpful to leach the salt in the unsaturated zone.

(3) The soil salt content and saturation on the surface had a significant response to the climate condition changes. It is very important to fully consider the seasonal climate variability for the future study of unsaturated soil salt distribution and transport. Further experiments on the combination of the numerical model and natural monitoring are needed to gain additional information on irrigation and drainage management. The use of Code_Bright in the investigation of solute transport in the unsaturated zone provides a theoretical basis for numerical analysis applications for coupled thermo-chemo-hydro–mechanical problems in agricultural engineering.

Author Contributions: Conceptualization, H.W. and R.C.; methodology, H.W. and R.C.; software, H.W.; validation, D.S. and R.C.; formal analysis, H.W.; investigation, H.W.; resources, D.S.; data curation, H.W.; writing—original draft preparation, H.W.; writing—review and editing, H.W.; visual-

ization, H.W.; supervision, D.S. and R.C.; project administration, H.W. and D.S.; funding acquisition, H.W. and D.S. All authors have read and agreed to the published version of the manuscript.

Funding: This study was financially supported by the National Natural Science Foundation of China through Grant No. 41825021 and No. 42307398, the Postdoctoral research initiation fee No. 423323, and the Natural Resources Science and Technology Project of Jiangsu Province No. 2022046.

Data Availability Statement: The data presented in this study are available on request from the first author.

Conflicts of Interest: The authors declare no conflict of interest.

References

1. Shackelford, C.D. Geoenvironmental Engineering. In *Reference Module in Earth Systems and Environmental Sciences*; Elsevier: Amsterdam, The Netherlands, 2013; pp. 1–29. [CrossRef]
2. Corwin, D.L. Climate change impacts on soil salinity in agricultural areas. *Eur. J. Soil Sci.* **2021**, *72*, 842–862. [CrossRef]
3. Singh, A. Salinization and drainage problems of agricultural land. *Irrig. Drain.* **2020**, *69*, 844–853. [CrossRef]
4. Iost, S.; Landgraf, D.; Makeschin, F. Chemical soil properties of reclaimed marsh soil from Zhejiang Province P.R. China. *Geoderma* **2007**, *142*, 245–250. [CrossRef]
5. Liu, C.; Xu, J.M.; Ding, N.F.; Fu, Q.L.; Guo, B.; Lin, Y.C.; Li, H.; Li, N. The effect of long-term reclamation on enzyme activities and microbial community structure of saline soil at Shangyu, China. *Environ. Earth Sci.* **2013**, *69*, 151–159. [CrossRef]
6. Tian, B.; Wu, W.; Yang, Z.; Zhou, Y. Drivers, trends, and potential impacts of long-term coastal reclamation in China from 1985 to 2010. *Estuar. Coast. Shelf Sci.* **2016**, *170*, 83–90. [CrossRef]
7. Li, S.; Luo, W.; Jia, Z.; Tang, S.; Chen, C. The effect of natural rainfall on salt leaching under watertable management. *L. Degrad. Dev.* **2018**, *29*, 1953–1961. [CrossRef]
8. Gran, M.; Carrera, J.; Massana, J.; Saaltink, M.W.; Olivella, S.; Ayora, C.; Lloret, A. Dynamics of water vapor flux and water separation processes during evaporation from a salty dry soil. *J. Hydrol.* **2011**, *396*, 215–220. [CrossRef]
9. Liu, D.; She, D.; Mu, X. Water flow and salt transport in bare saline-sodic soils subjected to evaporation and intermittent irrigation with saline/distilled water. *L. Degrad. Dev.* **2019**, *30*, 1204–1218. [CrossRef]
10. Yan, S.F.; Yu, S.E.; Wu, Y.B.; Pan, D.F.; She, D.L.; Ji, J. Seasonal Variations in Groundwater Level and Salinity in Coastal Plain of Eastern China Influenced by Climate. *J. Chem.* **2015**. [CrossRef]
11. Okur, B.; Örçen, N. *Chapter 12—Soil Salinization and Climate Change*; Prasad, M.N.V., Pietrzykowski, M., Eds.; Elsevier: Amsterdam, The Netherlands, 2020; pp. 331–350. [CrossRef]
12. He, B.; Cai, Y.; Ran, W.; Jiang, H. Spatial and seasonal variations of soil salinity following vegetation restoration in coastal saline land in eastern China. *Catena* **2014**, *118*, 147–153. [CrossRef]
13. Geng, X.; Boufadel, M.C. Numerical modeling of water flow and salt transport in bare saline soil subjected to evaporation. *J. Hydrol.* **2015**, *524*, 427–438. [CrossRef]
14. Zhang, C.; Li, L.; Lockington, D. Numerical study of evaporation-induced salt accumulation and precipitation in bare saline soils: Mechanism and feedback. *Water Resour. Res.* **2014**, *50*, 8084–8106. [CrossRef]
15. Yang, T.; Šimůnek, J.; Mo, M.; Mccullough-Sanden, B.; Shahrokhnia, H.; Cherchian, S.; Wu, L. Assessing salinity leaching efficiency in three soils by the HYDRUS-1D and -2D simulations. *Soil Tillage Res.* **2019**, *194*. [CrossRef]
16. Mao, W.; Zhu, Y.; Wu, J.; Ye, M.; Yang, J. Modelling the salt accumulation and leaching processes in arid agricultural areas with a new mass balance model. *J. Hydrol.* **2020**, *591*, 125329. [CrossRef]
17. Olivella, S.; Gens, A.; Carrera, J.; Alonso, E.E. Numerical formulation for a simulator (CODE_BRIGHT) for the coupled analysis of saline media. *Eng. Comput.* **1996**, *13*, 87–112. [CrossRef]
18. Dongli, S.; Dongdong, L.; Jiajia, M.; Agbna, G.H.D. Hydrological responses on saline-sodic soil slopes in a coastal reclamation area of China. *Catena* **2016**, *144*, 130–140. [CrossRef]
19. Liu, D.; She, D. Sodicity effects on hydrological processes of sodic soil slopes under simulated rainfall. *Hydrol. Process.* **2017**, *31*, 981–994. [CrossRef]
20. Wang, H.; She, D.; Fei, Y.; Tang, S. Synergic effects of biochar and polyacrylamide amendments on the mechanical properties of silt loam soil under coastal reclamation in China. *Catena* **2019**, *182*, 104152. [CrossRef]
21. van Genuchten, M.T. Closed-Form Equation for Predicting the Hydraulic Conductivity of Unsaturated Soils. *Soil Sci. Soc. Am. J.* **1980**, *44*, 892–898. [CrossRef]
22. Hersbach, H.; Bell, B.; Berrisford, P.; Biavati, G.; Horányi, A.; Muñoz Sabater, J.; Nicolas, J.; Peubey, C.; Radu, R.; Rozum, I.; et al. ERA5 Monthly Averaged Data on Single Levels from 1979 to Present, ERA5 Monthly Averaged Data on Single Levels from 1959 to Present. 2019. Available online: https://www.ecmwf.int/en/forecasts/dataset/ecmwf-reanalysis-v5 (accessed on 21 October 2023).
23. Rose, D.A.; Konukcu, F.; Gowing, J.W. Effect of watertable depth on evaporation and salt accumulation from saline groundwater. *Aust. J. Soil Res.* **2005**, *43*, 565–573. [CrossRef]

24. Ahmad, M.U.D.; Bastiaanssen, W.G.M.; Feddes, R.A. Sustainable use of groundwater for irrigation: A numerical analysis of the subsoil water fluxes. *Irrig. Drain.* **2002**, *51*, 227–241. [CrossRef]
25. Hunt, A.G.; Skinner, T.E.; Ewing, R.P.; Ghanbarian-Alavijeh, B. Dispersion of solutes in porous media. *Eur. Phys. J. B* **2011**, *80*, 411–432. [CrossRef]
26. Campbell, G.S.; Norman, J.M. *An Introduction to Environmental Biophysics, An Introduction to Environmental Biophysics*; Springer: New York, NY, USA, 1998. [CrossRef]
27. Yu, X.; Dan, H.-C.; Xin, P. Method for Improving Leaching Efficiency of Coastal Subsurface Drainage Systems. *J. Irrig. Drain. Eng.* **2018**, *144*, 04018019. [CrossRef]
28. Wang, S.; Song, X.; Wang, Q.; Xiao, G.; Wang, Z.; Liu, X.; Wang, P. Shallow groundwater dynamics and origin of salinity at two sites in salinated and water-deficient region of North China Plain, China. Environ. *Earth Sci.* **2012**, *66*, 729–739. [CrossRef]
29. Adrover, M.; Moyà, G.; Vadell, J. Seasonal and depth variation of soil chemical and biological properties in alfalfa crops irrigated with treated wastewater and saline groundwater. *Geoderma* **2017**, *286*, 54–63. [CrossRef]
30. Hongde, W.; Dongli, S.; Yipeng, Z.; Donghao, M. Unsaturated soil shear strength of agricultural soils influenced by reclaimed sequences in coastal China. *Eur. J. Soil Sci.* **2022**, *73*, e13237. [CrossRef]
31. Yang, Y.; Zhu, Y.; Wu, J.; Mao, W.; Ye, M.; Yang, J. Development and application of a new package for MODFLOW-LGR-MT3D for simulating regional groundwater and salt dynamics with subsurface drainage systems. *Agric. Water Manag.* **2022**, *260*, 107330. [CrossRef]
32. Eswar, D.; Karuppusamy, R.; Chellamuthu, S. Drivers of Soil Salinity and Their Correlation with Climate Change. *Curr. Opin. Env. Sustain.* **2021**, *50*, 310–318. [CrossRef]
33. Grieve, C.M.; Grattan, S.R.; Maas, E.V. Chapter 13 Plant Salt Tolerance. *Agric. Salin. Assess. Manag.* **2012**, *71*, 405–459. [CrossRef]

Disclaimer/Publisher's Note: The statements, opinions and data contained in all publications are solely those of the individual author(s) and contributor(s) and not of MDPI and/or the editor(s). MDPI and/or the editor(s) disclaim responsibility for any injury to people or property resulting from any ideas, methods, instructions or products referred to in the content.